Tunnel magnetoresistance in ferromagnetic junctions: Tunneling through a single discrete level

W. Rudziński[1] and J. Barnaś[1,2]
[1]*Department of Physics, Adam Mickiewicz University, ulica Umultowska 85, 61-614 Poznań, Poland*
[2]*Institute of Molecular Physics, Polish Academy of Sciences, ulica M. Smoluchowskiego 17, 60-179 Poznań, Poland*
(Received 3 March 2001; published 8 August 2001)

Tunnel magnetoresistance in a double-barrier junction with ferromagnetic electrodes, and a quantum dot (or a single atom) as the central part, is analyzed theoretically in the sequential-tunneling regime. The magnetoresistance is due to the rotation of magnetic moments of external electrodes from antiparallel to parallel alignment. The considerations are restricted to the case of a single discrete level, with Coulomb correlations and spin-flip transitions included. The tunneling current and occupation numbers are calculated for both magnetic configurations. It is shown that electron correlations at the dot can enhance the magnetoresistance effect, and give rise to a diodelike behavior. Spin-flip processes, on the other hand, suppress the magnetoresistance, and reduce the magnetically induced asymmetry in the current-voltage characteristics with respect to the bias reversal.

DOI: 10.1103/PhysRevB.64.085318 PACS number(s): 73.23.Hk, 73.40.Gk, 75.70.−i

I. INTRODUCTION

Electron tunneling in magnetic junctions is of current interest, due to expected applications of the tunnel magnetoresistance (TMR) effect. The key point of the phenomenon is the dependence of the tunnel resistance of ferromagnetic junctions on the relative orientation of the magnetic moments of external electrodes.[1] The effect is similar to the giant magnetoresistance effect in magnetic multilayers, where the resistance depends on the relative orientation of the magnetic moments of ferromagnetic films separated by nonmagnetic metallic layers.[2] The TMR effect exists in simple planar junctions as well as in more complex ones, such as, for instance, planar[3] or mesoscopic[4–6] double-barrier junctions, and junctions including granular systems.[7]

When the central electrode in mesoscopic double-barrier junctions is small (small capacitance C), then the charging energy $E_c=e^2/2C$ can be larger than the thermal energy k_BT, and can lead to Coulomb blockade of electric current below a certain threshold voltage. Apart from this, characteristic Coulomb steps in the current-voltage characteristics can then occur above the threshold voltage.[8,9] For sufficiently small central electrodes, the effects due to quantization of energy levels becomes visible as well. In this case, electrons tunnel through discrete levels.[10–12] In the case of ferromagnetic junctions, the limit of small level separation $\Delta E \ll E_c$ was studied theoretically in the sequential tunneling regime.[13–15] The opposite case $\Delta E \gg E_c$ was not analyzed—except in a simplified situation when electrons could tunnel through a single level in the strong correlation limit, when states with double occupancy were not involved.[16] There, it was shown that the tunneling current in a nonsymmetric junction is highly asymmetric with respect to the bias reversal, and in a certain bias range the junction can work as a diode.

In this paper we consider electron tunneling through a single discrete atomiclike level (quantum dot), for an arbitrary value of the correlation parameter U. In this case the double occupancy of the level is allowed. The considerations are restricted to the sequential tunneling limit. However, we take into account spin relaxation processes in the dot, which were neglected in Ref. 16. Such processes are very important, not only for the tunnel magnetoresistance, but also for the symmetry of the current-voltage characteristics and diodelike behavior. More specifically, we show that spin-flip processes at the dot can suppress the TMR effect, and also diminish or suppress the asymmetry of the current-voltage characteristics.

In Sec. II we describe the model and analyze the general situation, when the correlation parameter is arbitrary. Numerical results on the tunneling current and magnetoresistance in the general case are shown and discussed in Sec. III. Analytical and numerical results in the large-U limit are discussed in Sec. IV. Final conclusions and summary appear in Sec. V.

II. DESCRIPTION OF THE MODEL

We consider a junction in which a small central part is coupled to two ferromagnetic leads (electrodes) by tunneling barriers. The central part is so small that only a single discrete level is active in the tunneling processes. One may thus think of the central part as a semiconducting quantum dot with a single atomiclike level, or simply as an impurity located inside the barrier in the case of simple planar junctions. For simplicity, the central part will be referred to in the following as a dot. The tunneling current depends on the relative orientation of the magnetic moments of the external electrodes. To simplify the problem, we will consider only parallel and antiparallel configurations.

To describe the tunneling processes, we use the following model Hamiltonian of the junction:

$$H=H_l+H_r+H_d+H_t. \tag{1}$$

Here H_l and H_r describe the left and right electrodes in the noninteracting particle limit,

$$H_\nu=\sum_{nk\sigma}\epsilon^{\nu}_{nk\sigma}a^{+}_{\nu nk\sigma}a_{\nu nk\sigma}, \tag{2}$$

 ©2001 The American Physical Society

for $\nu=l$ and r, where $\epsilon^{\nu}_{nk\sigma}$ is the single-electron energy in the electrode ν for a one-dimensional wave vector k, a transverse channel n, and spin σ ($\sigma=\uparrow,\downarrow$), whereas $a^{+}_{\nu nk\sigma}$ and $a_{\nu nk\sigma}$ are the corresponding creation and destruction operators. The Hamiltonian H_d in Eq. (1) describes the central part (impurity or a dot), and is of the form

$$H_d=\epsilon_d\sum_{\sigma} c^{+}_{\sigma}c_{\sigma}+Un_{\uparrow}n_{\downarrow}+Rc^{+}_{\uparrow}c_{\downarrow}+R^{\star}c^{+}_{\downarrow}c_{\uparrow}, \tag{3}$$

where U is the electron correlation parameter for the dot; $n_{\sigma}=c^{+}_{\sigma}c_{\sigma}$ is the occupation operator, whereas R describes the spin-flip relaxation processes. Finally, H_t in Eq. (1) stands for the tunneling part of the Hamiltonian, and can be written as

$$H_t=\sum_{nk\sigma} T^{l}_{nk\sigma}a^{+}_{lnk\sigma}c_{\sigma}+\sum_{nk\sigma} T^{r}_{nk\sigma}a^{+}_{rnk\sigma}c_{\sigma}+\text{H.c.}, \tag{4}$$

where $T^{l}_{nk\sigma}$ and $T^{r}_{nk\sigma}$ are the tunneling parameters, and it was assumed that electron spin is conserved in the tunneling processes.

Our considerations are limited to the sequential tunneling regime. In this regime, the tunneling of an electron from source to drain electrodes is a sequence of two incoherent processes. To find the tunneling current in this regime, one can use the master equation method. It is worth noting that such a decription is valid when $k_BT\gg\Gamma$, where Γ is the width of the discrete level, and barrier resistances are larger than the quantum resistance.

Following the method developed by Glazman and Matweev,[17] we write

$$\frac{d}{dt}\langle n_{\sigma}\rangle=\Gamma^{+}_{\sigma}[1-\langle n_{\sigma}\rangle-\langle n_{-\sigma}\rangle+\langle n_{\uparrow}n_{\downarrow}\rangle]-\Gamma^{-}_{\sigma}[\langle n_{\sigma}\rangle-\langle n_{\uparrow}n_{\downarrow}\rangle]+\tilde{\Gamma}^{+}_{\sigma}[\langle n_{-\sigma}\rangle-\langle n_{\uparrow}n_{\downarrow}\rangle]-\tilde{\Gamma}^{-}_{\sigma}\langle n_{\uparrow}n_{\downarrow}\rangle-\frac{\langle n_{\sigma}\rangle-\langle n_{-\sigma}\rangle}{\tau_s} \tag{5a}$$

for $\sigma=\uparrow$ and $\sigma=\downarrow$, and

$$\frac{d}{dt}\langle n_{\uparrow}n_{\downarrow}\rangle=\tilde{\Gamma}^{+}_{\uparrow}[\langle n_{\downarrow}\rangle-\langle n_{\uparrow}n_{\downarrow}\rangle]-\tilde{\Gamma}^{-}_{\uparrow}\langle n_{\uparrow}n_{\downarrow}\rangle+\tilde{\Gamma}^{+}_{\downarrow}[\langle n_{\uparrow}\rangle-\langle n_{\uparrow}n_{\downarrow}\rangle]-\tilde{\Gamma}^{-}_{\downarrow}\langle n_{\uparrow}n_{\downarrow}\rangle. \tag{5b}$$

Here $\tau_s=2\tau_{sf}$, where τ_{sf} is the spin-relaxation time due to spin-flip transitions described by the parameter R of Hamiltonian (1), whereas Γ^{+}_{σ} (Γ^{-}_{σ}) describes the tunneling rate of electrons with spin σ, which tunnel to (from) the discrete level, when this level is not occupied. Similarly, $\tilde{\Gamma}^{+}_{\sigma}$ ($\tilde{\Gamma}^{-}_{\sigma}$) describes the tunneling rate of electrons with spin σ, which tunnel to (from) the discrete level, when the level is already occupied by an electron with spin $-\sigma$. These tunneling rates include tunneling through both barriers, and can be written as

$$\Gamma^{\pm}_{\sigma}=\Gamma^{\pm}_{l\sigma}+\Gamma^{\pm}_{r\sigma}\equiv f^{\pm}_{l}\gamma_{l\sigma}+f^{\pm}_{r}\gamma_{r\sigma}, \tag{6a}$$

$$\tilde{\Gamma}^{\pm}_{\sigma}=\tilde{\Gamma}^{\pm}_{l\sigma}+\tilde{\Gamma}^{\pm}_{r\sigma}\equiv\tilde{f}^{\pm}_{l}\tilde{\gamma}_{l\sigma}+\tilde{f}^{\pm}_{r}\tilde{\gamma}_{r\sigma}, \tag{6b}$$

where

$$\gamma_{\nu\sigma}=\frac{2\pi}{\hbar}\sum_{nk}|T^{\nu}_{nk\sigma}|^2\delta(\epsilon_d-\epsilon^{\nu}_{nk\sigma}), \tag{7a}$$

$$\tilde{\gamma}_{\nu\sigma}=\frac{2\pi}{\hbar}\sum_{nk}|T^{\nu}_{nk\sigma}|^2\delta(\epsilon_d+U-\epsilon^{\nu}_{nk\sigma}), \tag{7b}$$

and f^{+}_{ν} and $\tilde{f}^{+}_{\nu}$ are the Fermi distribution functions

$$f^{+}_{\nu}=\frac{1}{1+\exp[(\epsilon_d-\mu_{\nu})/k_BT]}, \tag{8a}$$

$$\tilde{f}^{+}_{\nu}=\frac{1}{1+\exp[(\epsilon_d+U-\mu_{\nu})/k_BT]}, \tag{8b}$$

whereas $f^{-}_{\nu}=1-f^{+}_{\nu}$ and $\tilde{f}^{-}_{\nu}=1-\tilde{f}^{+}_{\nu}$. In the above equations, μ_{ν} stands for the electrochemical potential of the lead ν.

Equations (5a) and (5b) determine the time dependence of the average occupation numbers. However, here we are interested in a stationary solution only, so these equations can be reduced further. In the following we change the notation $\langle n_{\uparrow}\rangle\Rightarrow n_{\uparrow}$, $\langle n_{\downarrow}\rangle\Rightarrow n_{\downarrow}$, and $\langle n_{\uparrow\downarrow}\rangle\Rightarrow n_{\uparrow\downarrow}$. Thus, in the stationary state, one may write

$$\Gamma^{+}_{\uparrow}(1-n_{\downarrow})-(\Gamma^{+}_{\uparrow}+\Gamma^{-}_{\uparrow})(n_{\uparrow}-n_{\uparrow\downarrow})+\tilde{\Gamma}^{+}_{\uparrow}n_{\downarrow}-(\tilde{\Gamma}^{+}_{\uparrow}+\tilde{\Gamma}^{-}_{\uparrow})n_{\uparrow\downarrow}-\frac{n_{\uparrow}-n_{\downarrow}}{\tau_s}=0, \tag{9a}$$

$$\Gamma^{+}_{\downarrow}(1-n_{\uparrow})-(\Gamma^{+}_{\downarrow}+\Gamma^{-}_{\downarrow})(n_{\downarrow}-n_{\uparrow\downarrow})+\tilde{\Gamma}^{+}_{\downarrow}n_{\uparrow}-(\tilde{\Gamma}^{+}_{\downarrow}+\tilde{\Gamma}^{-}_{\downarrow})n_{\uparrow\downarrow}-\frac{n_{\downarrow}-n_{\uparrow}}{\tau_s}=0, \tag{9b}$$

$$\tilde{\Gamma}^{+}_{\uparrow}n_{\downarrow}-(\tilde{\Gamma}^{+}_{\uparrow}+\tilde{\Gamma}^{-}_{\uparrow})n_{\uparrow\downarrow}+\tilde{\Gamma}^{+}_{\downarrow}n_{\uparrow}-(\tilde{\Gamma}^{+}_{\downarrow}+\tilde{\Gamma}^{-}_{\downarrow})n_{\uparrow\downarrow}=0. \tag{9c}$$

From Eqs. (9a)–(9c), one can find all the occupation numbers. These numbers allow us to calculate the tunneling current flowing through the system. Due to the charge conservation, the current flowing in the stationary state through the left barrier is equal to that flowing through the right barrier. One may thus write

$$I=e\sum_{\sigma}[\Gamma^{-}_{r\sigma}(n_{\sigma}-n_{\uparrow\downarrow})-\Gamma^{+}_{r\sigma}(1-n_{\sigma}-n_{-\sigma}+n_{\uparrow\downarrow})]+e\sum_{\sigma}[\tilde{\Gamma}^{-}_{r\sigma}n_{\uparrow\downarrow}-\tilde{\Gamma}^{+}_{r\sigma}(n_{-\sigma}-n_{\uparrow\downarrow})]. \tag{10}$$

Taking into account Eqs. (6a) and (6b), this formula may be rewritten as

$$I=e\sum_{\sigma}\{\gamma_{r\sigma}[n_{\sigma}-n_{\uparrow\downarrow}-f_r^{+}(1-n_{-\sigma})]+\tilde{\gamma}_{r\sigma}(n_{\uparrow\downarrow}-\tilde{f}_r^{+}n_{-\sigma})\}. \tag{11}$$

When the effects due to band structure can be neglected by assuming a constant density of states and constant tunneling matrix elements, then one may write

$$\tilde{\gamma}_{\nu\sigma}=\gamma_{\nu\sigma} \tag{12}$$

for $\nu=l$ and $\nu=r$. In this case, formula (11) for the tunneling current can be rewritten as

$$I=e\sum_{\sigma}\gamma_{r\sigma}[n_{\sigma}-f_r^{+}(1-n_{-\sigma})-\tilde{f}_r^{+}n_{-\sigma}]. \tag{13}$$

Using Eq. (13), one can calculate tunneling current for both magnetic configurations, and consequently also the tunnel magnetoresistance. Below we describe some numerical results.

III. NUMERICAL RESULTS

The effects considered in this paper follow from the spin dependence of the tunneling processes described by the parameters $\Gamma_{l\sigma}^{\pm}$, $\Gamma_{r\sigma}^{\pm}$, $\tilde{\Gamma}_{l\sigma}^{\pm}$, and $\tilde{\Gamma}_{r\sigma}^{\pm}$. For simplicity, we will neglect all effects following from the band structure, and assume $\gamma_{\nu\sigma}=\tilde{\gamma}_{\nu\sigma}$. To describe the spin dependence more quantitatively, we introduce the spin asymmetry factors p_l and p_r for the left and right barriers, respectively,

$$\gamma_{l\pm}=\gamma_0(1\pm p_l), \tag{14a}$$

$$\gamma_{r\pm}=\alpha\gamma_0(1\pm p_r), \tag{14b}$$

where the upper (lower) sign is for the spin-majority ($\sigma=+$) and spin-minority ($\sigma=-$) electrons, and γ_0 is a parameter. In the following we assume that γ_0 is independent of the bias voltage. In Eq. (14b), we additionally introduced the factor α, which describes the asymmetry between the right and left barriers. Equations (14a) and (14b) are written in the local quantization axes (along the local magnetization direction). According to our notation, the spin orientations in the global quantization axis are described by $\uparrow$ and $\downarrow$.

We will consider two magnetic configurations—parallel and antiparallel configurations. We also assume that in the antiparallel configuration the magnetization of the right electrode is reversed. Thus one can write

$$\gamma_{r\uparrow(\downarrow)}=\alpha\gamma_0(1\pm p_r) \tag{15a}$$

for the parallel configuration, and

$$\gamma_{r\uparrow(\downarrow)}=\alpha\gamma_0(1\mp p_r) \tag{15b}$$

for the antiparallel one.

Another parameter introduced to describe numerical results is the dimensionless frequency Ω, defined as

$$\Omega=\frac{1}{\gamma_0\tau_s}. \tag{16}$$

Physically, Ω is related to the ratio of the spin-flip and tunneling rates. Thus $\Omega=0$ corresponds to the limit of no spin relaxation, while large values of Ω, $\Omega\gg1$, correspond to the case of fast spin relaxation.

We assume that the positive bias corresponds to the case when electrons flow from the left to right reservoires. An important question now is how the discrete level ϵ_d varies with the bias voltage V. If we measure the energy from the Fermi level of the left electrode ($\mu_l=0$), then $\mu_r=-eV$, and we assume that $\epsilon_d=\epsilon_d^0-xeV$, where $0<x<1$, and ϵ_d^0 denotes the energy of the discrete level in equilibrium ($V=0$). In real situations the value of the parameter x depends on the barriers on both sides of the dot, and also on the charge accumulated on the dot. If we assume a linear drop of the electrostatic potential between the electrodes, then one may write $x=d_l/(d_l+d_r)$, where d_l and d_r denote the thicknesses of the left and right barriers, respectively. Such a simplified description, however, neglects the shift of the level position due to electrostatic potential of the charged dot.[18]

From Eqs. (9a)–(9c), it follows that the occupation numbers $n_{\uparrow}$, $n_{\downarrow}$, and $n_{\uparrow\downarrow}$ depend on the tunneling rate γ_0 and relaxation time τ_s only via the parameter Ω. The electric current, on the other hand, depends on γ_0 and τ_s through the occupation numbers, and also through a factor linear in γ_0. Therefore, it is convenient to normalize current to $e\gamma_0$.

A. Symmetrical junctions

First consider a symmetrical junction, i.e., the case when both barriers are identical: $p_l=p_r$, $\alpha=1$, and $x=1/2$. Let us neglect, for a while, spin-flip relaxation processes on the dot. Since now $I(-V)=-I(V)$, the analysis will be restricted to positive bias only, $V>0$. Figure 1(a) shows typical variations of the occupation numbers $n_{\uparrow}$ and $n_{\downarrow}$ with the bias voltage V, calculated for both parallell and antiparallel configurations. In both cases, the first step in $n_{\uparrow}$ and $n_{\downarrow}$ occurs at the bias, when the discrete level ϵ_d crosses the Fermi level of the left (source) electrode. On the other hand, the step at a higher voltage corresponds to the case when ϵ_d+U crosses this Fermi level. Figure 1(b) shows $n_{\uparrow\downarrow}$ for both magnetic configurations. Note that there is only one step in $n_{\uparrow\downarrow}$, which occurs at a voltage corresponding to the second step in $n_{\uparrow}$ and $n_{\downarrow}$. It is also interesting to note that in the parallel configuration $n_{\uparrow}=n_{\downarrow}$, whereas in the antiparallel configuration $n_{\uparrow}\neq n_{\downarrow}$. The situation is similar to that in the case of symmetrical junctions with large central electrodes (islands), where difference in spin asymmetry for tunneling rates across the left and right barriers (which takes place in the antiparallel configuration only) gives rise to a spin split of the island Fermi level, and consequently leads to spin accumulation.[5,15] No such effect occurs when the spin asymmetry for both barriers is the same, which for symmetrical junctions occurs only in the parallel configuration.

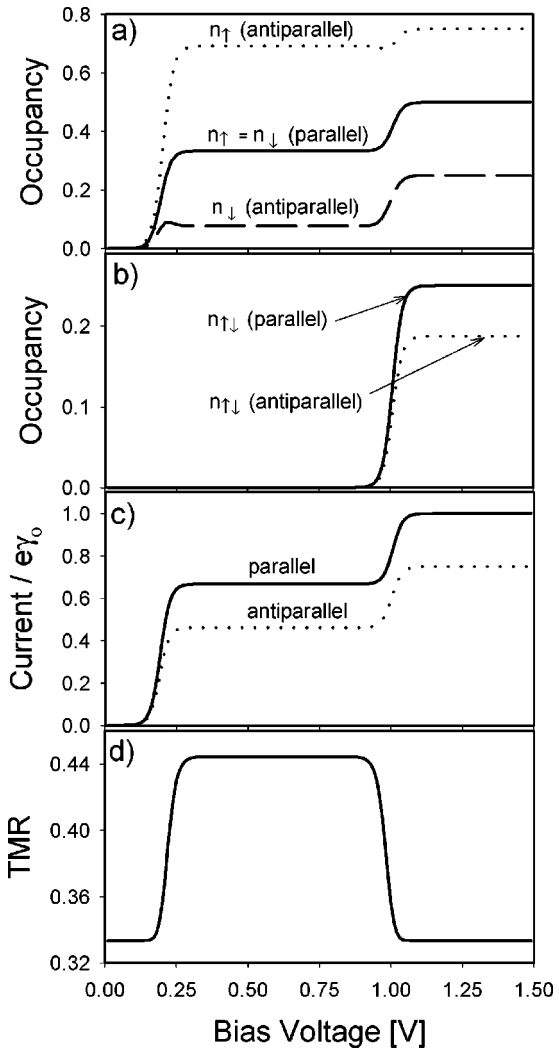

FIG. 1. Occupation numbers $n_\uparrow$ and $n_\downarrow$ (a), $n_{\uparrow\downarrow}$ (b), electric current (c), and TMR (d) in a symmetrical junction, calculated for no spin-flip processes. The other parameters are $\epsilon_d^0=0.1$ eV, $p_l=p_r=0.5$, $U=0.4$ eV, $\alpha=1$, $T=100$ K, and $x=0.5$.

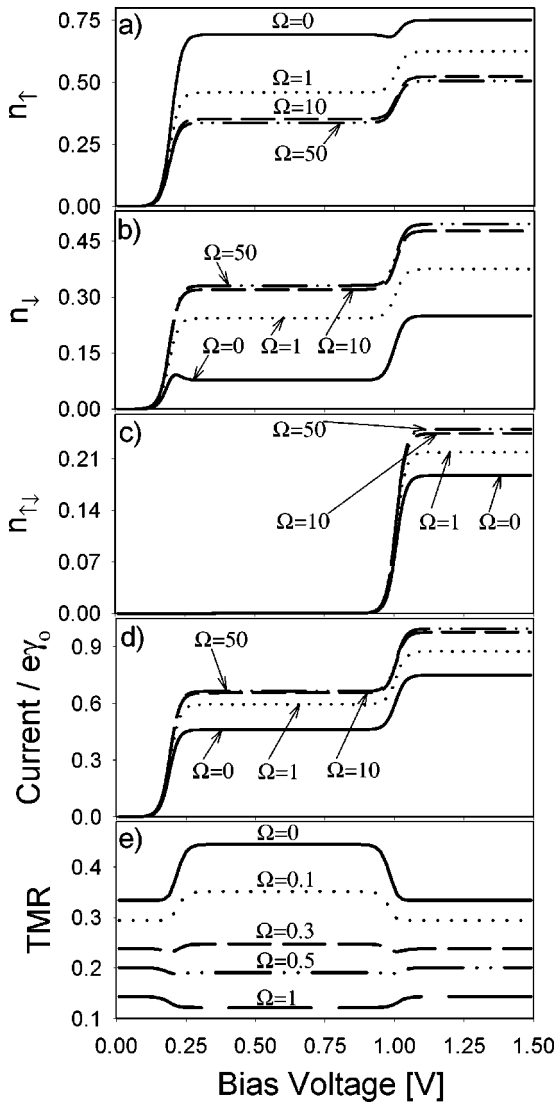

FIG. 2. Occupation numbers $n_\uparrow$ (a), $n_\downarrow$ (b), $n_{\uparrow\downarrow}$ (c), electric current (d), and TMR (e) calculated for different spin-flip rates, described by the indicated values of the parameter Ω. Parts (a)–(d) are calculated for the antiparallel configuration. The other parameters are as in Fig. 1.

Figure 1(c) shows the tunneling current calculated for both magnetic configurations and normalized to $e\gamma_0$. There are two steps in the current, which correspond to the steps in the occupation numbers $n_\uparrow$ and $n_\downarrow$, whereas between the steps the current is constant. At each step a new channel for tunneling becomes open. Figure 1(d) shows the corresponding tunnel magnetoresistance, defined quantatively as

$$\mathcal{T} \equiv \frac{R_{\rm ap}-R_{\rm p}}{R_{\rm p}} = \frac{I_{\rm p}-I_{\rm ap}}{I_{\rm ap}}, \tag{17}$$

where $R_{\rm ap}$ and $R_{\rm p}$ denote the total junction resistance in the antiparallel and parallel configurations, respectively. The magnetoresistance is significantly enhanced in the bias range bounded by the voltages corresponding to the two steps in the occupation numbers (as well as in the current).

Let us now consider the influence of spin-flip transitions at the dot on the tunneling characteristics. Generally, one may expect that spin-flip transitions reduce the difference between $n_\uparrow$ and $n_\downarrow$. Since $n_\uparrow=n_\downarrow$ for $\Omega=0$ (no spin-flip processes) in the parallel configuration, the spin-flip processes have no influence on the occupation numbers in this geometry. Moreover, because electric current depends on the spin-flip transitions implicitly through the occupation numbers, the electric current in the parallel configuration is also insensitive to the parameter Ω. The situation is different in the antiparallel configuration, where $n_\uparrow \neq n_\downarrow$ for $\Omega=0$ [see Fig. 1(a)]. Thus the difference between $n_\uparrow$ and $n_\downarrow$ should decrease with increasing Ω. Indeed, this is the case as shown in Figs. 2(a) and 2(b), where the occupation numbers $n_\uparrow$ and $n_\downarrow$ are presented for different values of the parameter Ω. One can note that $n_\uparrow$ and $n_\downarrow$ tend to the same value with increasing Ω, which coincides with $n_\uparrow=n_\downarrow$ in the parallel configuration. Also, the value of $n_{\uparrow\downarrow}$ in the antiparallel configuration varies with increasing Ω [see Fig. 2(c)] approaching the corresponding value in the parallel configuration.

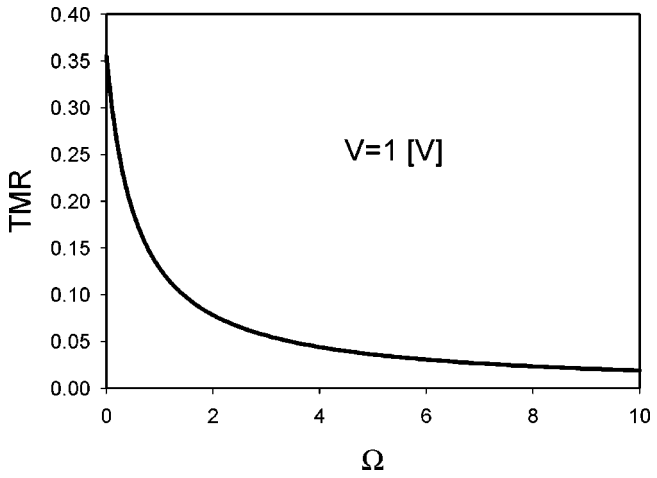

FIG. 3. TMR as a function of the parameter Ω, calculated for $V=1$ V. The other parameters are as in Fig. 1.

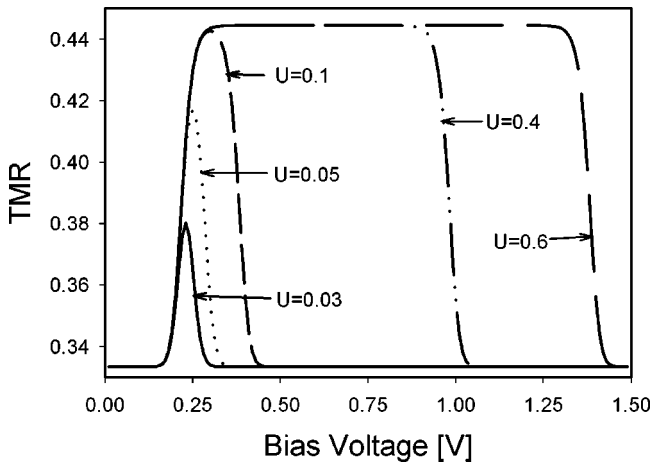

FIG. 4. TMR as a function of the bias voltage, calculated for indicated values of the correlation parameter U. The other parameters are as in Fig. 1.

Figure 2(d) shows the influence of the spin-relaxation processes on the tunneling current in the antiparallel configuration. With increasing Ω, the current tends to the current flowing in the parallel configuration [compare with Fig. 1(c)].

The TMR effect is shown in Fig. 2(e) for a few values of Ω. Generally, TMR decreases with increasing Ω, i.e., with decreasing spin-relaxation time. This is clearly visible in Fig. 2(e), where the curves describing TMR move down when Ω increases. Apart from this, the broad and flat maximum in TMR disappears above a certain value of Ω. To see how fast TMR disappears with increasing Ω, in Fig. 3 we show explicitly the Ω dependence of TMR for a particular voltage V. One can see that the main drop of TMR is for Ω ranging from $\Omega=0$ to $\Omega\approx 1$. For $\Omega>1$, TMR is rather small, and decreases further with increasing Ω.

As follows from Fig. 1(d), the TMR effect at $\Omega=0$ is enhanced by Coulomb correlations, when the voltage is in the range limited by the voltages corresponding to the two steps in the current-voltage characteristics. An interesting question is what happens when the correlation parameter U decreases and finally disappears. This is shown in Fig. 4, where TMR is presented for different values of the correlation parameter U. The broad and flat maximum in TMR becomes narrower with decreasing value of U, but its height remains unchanged when the parameter U is not too small. At sufficiently small values of U, height of the peak in TMR decreases, vanishing finally when $U\rightarrow 0$. Thus, one may state that Coulomb correlations on the dot can lead to an enhanced TMR in a certain bias range.

B. Asymmetrical junction

Consider now an asymmetrical situation, $\alpha\neq 1$ and $p_l \neq p_r$. For numerical calculations we assume $p_l=0.4$, $p_r=0.9$, and $\alpha=0.1$. For positive bias, the assumed parameters correspond to the situation when the matrix elements for tunneling from the dot to the drain electrode are strongly spin dependent, much more strongly than the matrix elements for tunneling from the source electrode to the dot. This difference also gives rise to the difference in the occupation numbers in the parallel configuration, $n_\uparrow \neq n_\downarrow$. The factor $\alpha=0.1$, on the other hand, indicates that on average electrons can tunnel much easier to the dot than out of it. Thus electrons which have tunneled to the dot prevent other electrons of the source electrode from tunneling onto it. The situation is different for negative bias, when electrons flow from the right to the left. Now the larger spin asymmetry in tunneling matrix elements is for electrons tunneling to the dot. This should also give rise to a difference in the occupation numbers in the parallel configuration, but of opposite sign. Moreover, it is now much easier on average for electrons to tunnel out of the dot than to the dot. This means that electrons which have tunneled onto the dot through the right barrier leave the dot rather quickly through the left barrier, and therefore have no significant influence on the subsequent tunneling processes.

The asymmetry between the left and right electrodes and barriers gives rise to asymmetrical characteristics of the junctions with respect to the change of the bias sign. Figure 5 shows a variation of the occupation numbers in the parallel configuration with the bias voltage V, calculated for different values of the parameter Ω, which range from the slow to fast spin relaxation limits. Consider, first, the case of positive bias and no spin relaxation: $\Omega=0$. The number of tunneling processes significantly increases at a voltage corresponding to the first step. Thus the occupation numbers $n_\uparrow$ and $n_\downarrow$ begin to increase at this voltage as well. When $n_\downarrow$ becomes larger than 0.5, then a further increase in $n_\downarrow$ results in a decrease in $n_\uparrow$, as one can conclude from Figs. 5(a) and 5(b). This gives rise to the peak in $n_\uparrow$ at voltages in the vicinity of the first step. Since now $p_l\neq p_r$, then $n_\uparrow\neq n_\downarrow$, not only in the antiparallel confuration but also in the parallel one, as already discussed above. For the parameters assumed in Fig. 5, electrons with spin $\sigma=\uparrow$ tunnel easier to the dot than electrons with spin $\sigma=\downarrow$. A similar situation also takes place for electrons tunneling from the dot to the drain electrode,

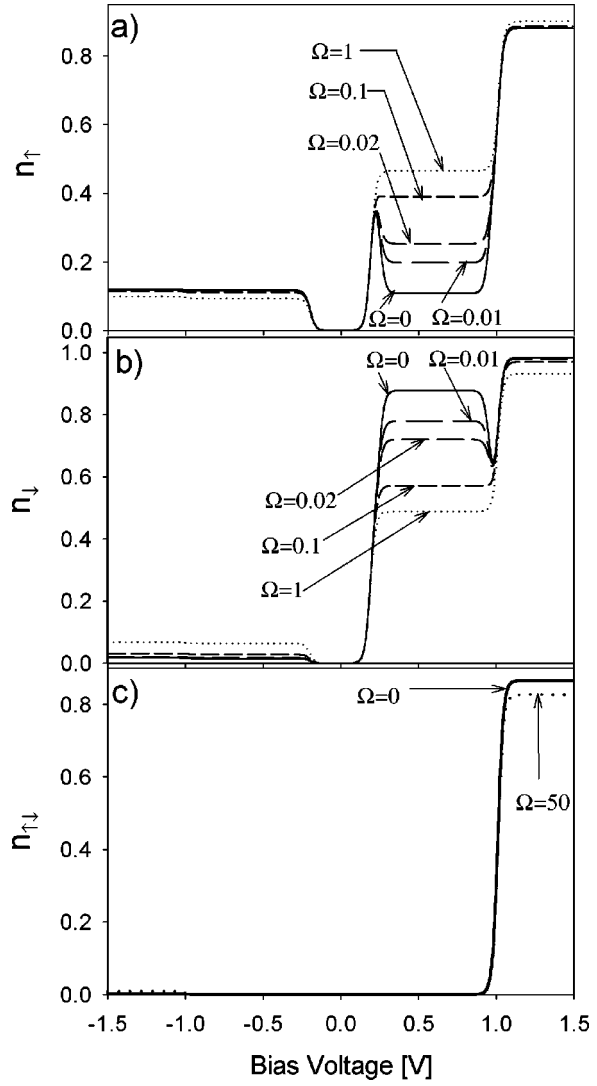

FIG. 5. Occupation numbers $n_\uparrow$ (a), $n_\downarrow$ (b), and $n_{\uparrow\downarrow}$ (c) in an asymmetrical junction in the parallel configuration and for different spin-flip rates, described by the indicated values of the parameter Ω. The other parameters are $\epsilon_d^0=0.1$ eV, $p_l=0.4$, $p_r=0.9$, $U=0.4$ eV, $\alpha=0.1$, $T=100$ K, and $x=0.5$.

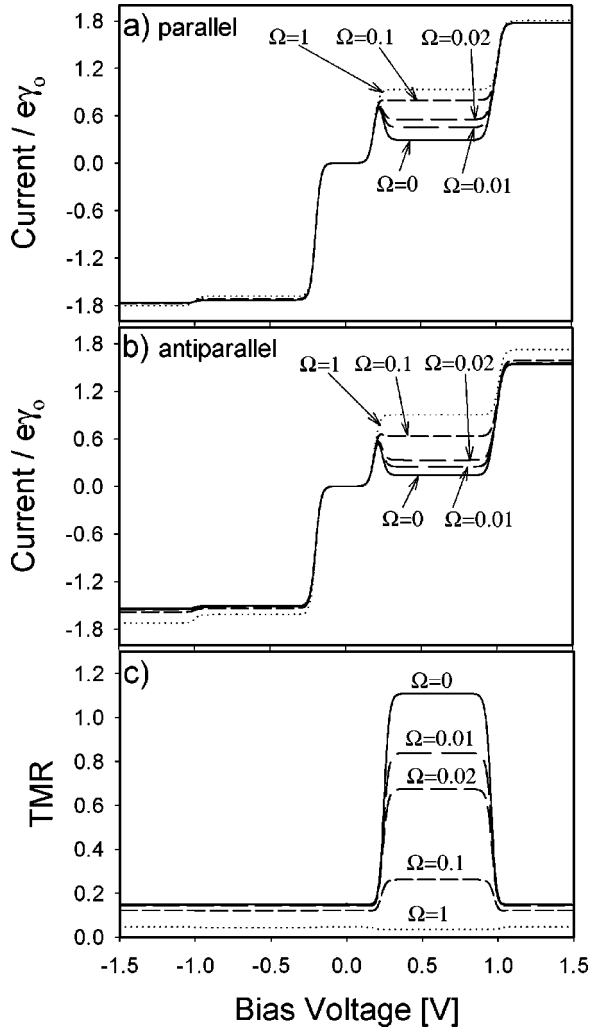

FIG. 6. Electric current in the parallel (a) and antiparallel (b) configurations, and TMR (c) calculated for different spin-flip rates, described by the indicated values of the parameter Ω. The other parameters are as in Fig. 5.

but now the spin asymmetry is much larger. Consequently, $n_\downarrow > n_\uparrow$ and the flowing current produces a net magnetic moment on the dot. When the bias approaches a value corresponding to the second step, then a new tunneling channel becomes open—mainly for electrons with spin $\sigma=\uparrow$. This results in a fast increase in $n_\uparrow$, and consequently in a decrease (dip) in $n_\downarrow$ for voltages close to the second step. Finally, at higher voltages, two electrons with opposite spin orientations can reside on the dot, and $n_\downarrow \approx n_\uparrow$. The number $n_{\uparrow\downarrow}$, shown in Fig. 5(c), behaves similarly to what occurs in the symmetrical case discussed above. The situation is significantly different for negative bias. Now the induced magnetic moment on the dot has an opposite sign, $n_\downarrow < n_\uparrow$, as already mentioned above. Apart from this, electrons now spend a much shorter time on the dot, so the values of $n_\uparrow$ and $n_\downarrow$ are rather small, much smaller than for positive bias. Another consequence of this is a very small value of $n_{\uparrow\downarrow}$.

If we include spin-relaxation processes, then the peak in $n_\uparrow$ in the vicinity of the first step and the dip in $n_\downarrow$ in the vicinity of the second step slowly disappear with increasing Ω, as is clearly evident in Figs. 5(a) and 5(b). Moreover, the difference in the occupation numbers $n_\uparrow$ and $n_\downarrow$ also disappears.

Figure 6 shows tunneling current in both magnetic configurations and TMR for different values of the parameter Ω. Consider, first, the situation when $\Omega=0$, i.e., for no spin-flip processes. An important property of the current-voltage curves is their strong asymmetry with respect to the bias reversal. For positive bias the electric current first increases with increasing bias, and then drops to a certain small value, which is almost independent of the bias, until V reaches the value corresponding to the second step, where the current increases relatively quickly and saturates at a certain level. The decrease of electric current at the voltage slightly above

the first step is caused by less conducting electrons with spin $\sigma=\downarrow$ residing on the dot, which block tunneling of the more conducting spin-$\uparrow$ electrons, as already discussed above. In the extreme limit of the half-metallic right electrode, $p=1$,the current above the maximum drops to zero, being totally blocked by an electron with spin $\sigma=\downarrow$ residing on the dot, and then rapidly increases when the bias reaches a value corresponding to the second step. For negative bias, on the other hand, the electric current reaches a maximum value right above the bias corresponding to the first step, and is roughly constant at higher voltages. Now electrons spend a much shorter time on the dot, and consequently electrons with a particular spin orientation have only a small influence on the tunneling of electrons with opposite spins.

When the spin-relaxation processes occur, then the situation changes significantly. For positive bias, the plateau between the peak in current and the second step moves up, and finally the peak at the first step disappears. For negative bias, on the other hand, the spin-flip processes have only a small influence on the electric current in both magnetic configurations. It is interesting to note that, even in the limit of fast spin relaxation on the dot, a certain asymmetry of the current-voltage characteristics survives. For positive bias there are then two clear steps, whereas for negative bias the first step is large while the second step is rather small.

The situation in the antiparallel configuration is qualitatively similar, but with the electron spins interchanged. Therefore, we will not discuss this configuration in more detail. The difference between currents flowing in both magnetic configurations gives rise to the TMR shown in Fig. 6(c). For $\Omega=0$ and for positive bias, there is a broad and flat maximum in TMR for voltages between the two steps. The behavior of this maximum, with an increasing value of the parameter Ω, is similar to that in the symmerical case, so we will not discuss it further here. However, it is very interesting to note that the enhancement of TMR by the correlation effects takes place only for positive bias. For negative bias, TMR remains almost constant and rather small. This is due to the fact that for negative bias the correlations play a minor role, since now $n_{\uparrow\downarrow}$ is very small. When the parameter Ω increases, then the difference between the occupation numbers and electric currents in both magnetic configurations becomes smaller, and finally disappears in the limit of fast spin relaxation. So does the TMR effect.

The influence of the parameter U on electric current and TMR is shown in Fig. 7 for the case of no spin relaxation, $\Omega=0$, and for positive bias only. When $U\to 0$, the second step in the current moves toward lower voltages, leaving the magnitude of the current above and below this step unchanged. In this limit the suppression of electric current above the first step (equivalent to the second step) disappears and TMR is constant, i.e., independent of the bias voltage.

IV. EMPTY LEVEL IN THE LARGE-U LIMIT

Now consider the case when, in equilibrium, the discrete level ϵ_d is slightly above the Fermi level, whereas ϵ_d+U is far above the Fermi level. In this case the level cannot be doubly occupied, $n_{\uparrow\downarrow}=0$, so $\tilde{f}_\nu^+\simeq 0$ and $\tilde{f}_\nu^-\simeq 1$ for $U\gg k_BT$ and $U\gg eV$. Only empty and singly occupied states are now involved in tunneling processes.

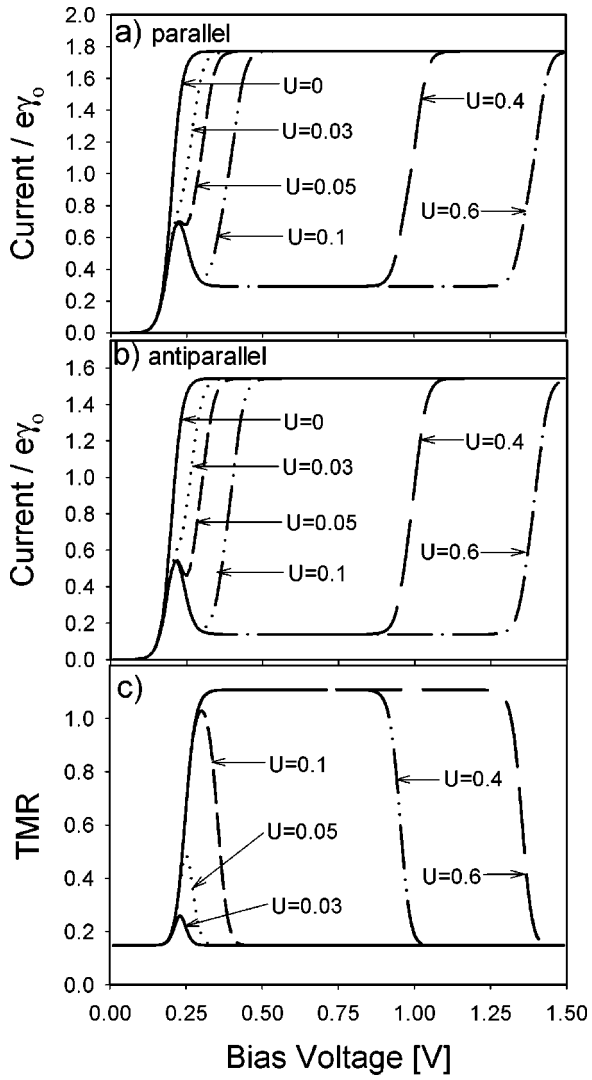

FIG. 7. Electric current in the parallel (a) and antiparallel (b) configurations and TMR (c), plotted as a function of the bias voltage for indicated values of the correlation parameter U. The other parameters are as in Fig. 5.

Equations (9a)–(9c) now reduce to the following:

$$\Gamma_\uparrow^+(1-n_\downarrow)-(\Gamma_\uparrow^++\Gamma_\uparrow^-)n_\uparrow-\frac{n_\uparrow-n_\downarrow}{\tau_s}=0, \qquad (18a)$$

$$\Gamma_\downarrow^+(1-n_\uparrow)-(\Gamma_\downarrow^++\Gamma_\downarrow^-)n_\downarrow-\frac{n_\downarrow-n_\uparrow}{\tau_s}=0. \qquad (18b)$$

A solution of these equations gives

$$n_{\uparrow}=\frac{\Gamma_{\uparrow}^{+}\Gamma_{\downarrow}^{-}\tau_s+\Gamma_{\uparrow}^{+}+\Gamma_{\downarrow}^{+}}{[(\Gamma_{\uparrow}^{+}+\Gamma_{\uparrow}^{-})(\Gamma_{\downarrow}^{+}+\Gamma_{\downarrow}^{-})-\Gamma_{\uparrow}^{+}\Gamma_{\downarrow}^{+}]\tau_s+2\Gamma_{\uparrow}^{+}+2\Gamma_{\downarrow}^{+}+\Gamma_{\uparrow}^{-}+\Gamma_{\downarrow}^{-}}, \tag{19a}$$

$$n_{\downarrow}=\frac{\Gamma_{\downarrow}^{+}\Gamma_{\uparrow}^{-}\tau_s+\Gamma_{\downarrow}^{+}+\Gamma_{\uparrow}^{+}}{[(\Gamma_{\uparrow}^{+}+\Gamma_{\uparrow}^{-})(\Gamma_{\downarrow}^{+}+\Gamma_{\downarrow}^{-})-\Gamma_{\uparrow}^{+}\Gamma_{\downarrow}^{+}]\tau_s+2\Gamma_{\uparrow}^{+}+2\Gamma_{\downarrow}^{+}+\Gamma_{\uparrow}^{-}+\Gamma_{\downarrow}^{-}}. \tag{19b}$$

The electric current can be then calculated from the formula

$$I=e\sum_{\sigma}\ \gamma_{r\sigma}[n_{\sigma}-f_r^{+}(1-n_{-\sigma})]. \tag{20}$$

Such a situation was considered in Ref. 16, in the limit of no spin-flip transitions. It was shown there that, when one of the electrodes is half-metallic (full spin polarization of electrons at the Fermi level), the junction may act as a diode. The current can flow, say, for negative bias, while for positive bias it can flow only in a certain region of the applied voltage. Here we consider the same parameters as in Ref. 16, and analyze in detail how the spin-flip transitions modify the junction characteristics. In Figs. 8(a) and 8(b) we show current in both magnetic configurations and for positive bias only. For $\Omega=0$ the current flows only in a small bias range around the voltage corresponding to the first step in the general case (see Fig. 1). This corresponds to the situation when the discrete level crosses the Fermi level of the source electrode. At higher voltages the current is suppressed. For one spin orientation, the electron which has tunneled to the discrete level cannot tunnel further, because there are no states available for it in the half-metallic drain electrode. This electron blocks the tunneling of other electrons. When the discrete level is close to the Fermi level of the source electrode, the current can flow, because the thermal distribution allows tunneling back to the source electrode, so that the discrete level becomes accessible for those electrons of the source electrode, which can tunnel to the drain electrode. For higher voltages, an individual electron, with a spin orientation for which the density of states in the drain electrode vanishes, is trapped in the level, and thus suppresses electric current. This takes place in both magnetic configurations. It is easy to conclude that this mechanism does not work for negative bias. In this case the current is not blocked.

The efficiency of the mechanism described above relies on the fact that the spin orientation of the trapped electron is conserved for a long time. Any spin-flip scattering will free the electron trapped in the dot, and allow it to tunnel further. Thus the diodelike behavior should strongly depend on the spin-flip transitions in the discrete level. Indeed this is the case, as shown in Figs. 8(a) and 8(b), where for $\Omega\approx 1$ the suppression of electric current disappears.

Differences in the current for parallel and antiparallel configurations give rise to TMR, shown in Fig. 8(c). The behavior of TMR with increasing Ω is qualitatively similar to that described for symmetrical junctions, so we will not discuss this point in more detail.

V. DEEP LEVEL IN THE LARGE-U LIMIT

Now consider the situation when the discrete level ϵ_d is far below the Fermi level, while ϵ_d+U is slightly above the Fermi level in equilibrium. In this case the level is always occupied with a single electron for $U\gg k_BT$ and $U\gg eV$, so $f_{\nu}^{+}\simeq 1$ and $f_{\nu}^{-}\simeq 0$. Only singly or doubly occupied states are

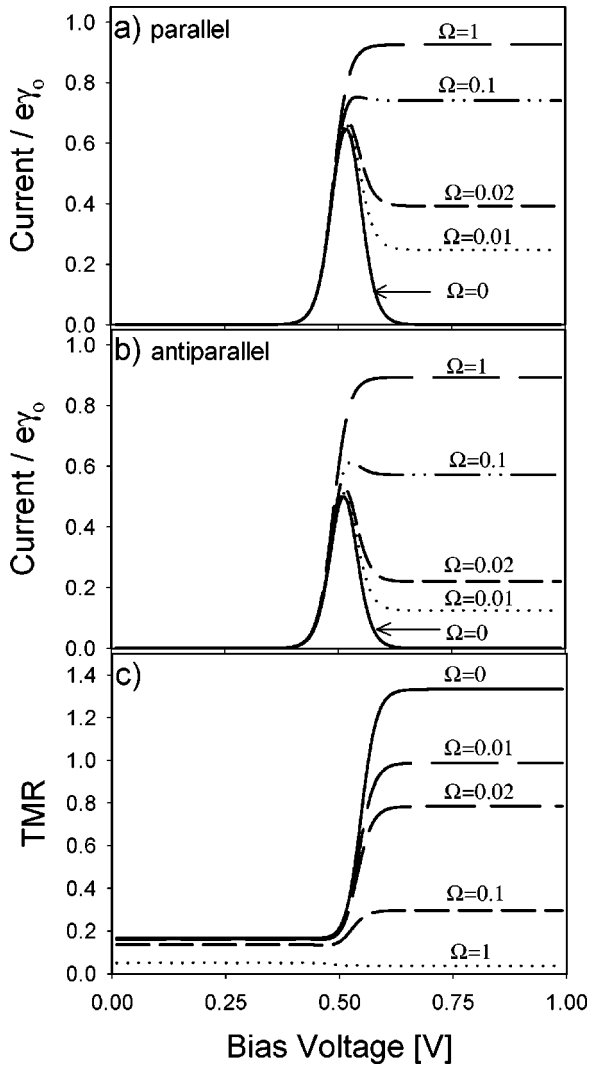

FIG. 8. Electric current in the parallel (a) and antiparallel (b) configurations, and TMR (c) as a function of the bias voltage, calculated for large-U limit with empty state in equilibrium. Different curves correspond to different spin-flip rates, described by the indicated values of the parameter Ω. The other parameters are $\epsilon_d^0=0.25$ eV, $p_l=0.4$, $p_r=1$, $\alpha=0.1$, $T=100$ K, and $x=0.5$.

involved in the tunneling processes. In this situation the expected value of zero occupancy vanishes,

$$\langle (1-n_\uparrow)(1-n_\downarrow)\rangle = 0, \tag{21}$$

or, equivalently,

$$n_\uparrow + n_\downarrow - n_{\uparrow\downarrow} = 1. \tag{22}$$

Equations (9a)–(9c) now reduce to the following:

$$\tilde{\Gamma}^+_\uparrow n_\downarrow - (\tilde{\Gamma}^+_\uparrow + \tilde{\Gamma}^-_\uparrow) n_{\uparrow\downarrow} - \frac{n_\uparrow - n_\downarrow}{\tau_s} = 0, \tag{23a}$$

$$\tilde{\Gamma}^+_\downarrow n_\uparrow - (\tilde{\Gamma}^+_\downarrow + \tilde{\Gamma}^-_\downarrow) n_{\uparrow\downarrow} - \frac{n_\downarrow - n_\uparrow}{\tau_s} = 0. \tag{23b}$$

These two equations, together with condition (22), allow one to calculate $n_\uparrow$, $n_\downarrow$, and $n_{\uparrow\downarrow}$. The results are

$$n_\uparrow = \frac{(\tilde{\Gamma}^+_\uparrow + 1/\tau_s)(\tilde{\Gamma}^+_\downarrow + \tilde{\Gamma}^-_\downarrow)\tau_s + (\tilde{\Gamma}^+_\uparrow + \tilde{\Gamma}^-_\uparrow)}{(\tilde{\Gamma}^+_\uparrow + 1/\tau_s)(\tilde{\Gamma}^+_\downarrow + 1/\tau_s)\tau_s - 1/\tau_s} n_{\uparrow\downarrow}, \tag{24a}$$

$$n_\downarrow = \frac{(\tilde{\Gamma}^+_\downarrow + 1/\tau_s)(\tilde{\Gamma}^+_\uparrow + \tilde{\Gamma}^-_\uparrow)\tau_s + (\tilde{\Gamma}^+_\downarrow + \tilde{\Gamma}^-_\downarrow)}{(\tilde{\Gamma}^+_\downarrow + 1/\tau_s)(\tilde{\Gamma}^+_\uparrow + 1/\tau_s)\tau_s - 1/\tau_s} n_{\uparrow\downarrow}, \tag{24b}$$

with

$$n_{\uparrow\downarrow} = \left\{ \frac{(\tilde{\Gamma}^+_\downarrow \tau_s + 1)(\tilde{\Gamma}^+_\uparrow + \tilde{\Gamma}^-_\uparrow) + (\tilde{\Gamma}^+_\downarrow + \tilde{\Gamma}^-_\downarrow)}{(\tilde{\Gamma}^+_\downarrow \tau_s + 1)\tilde{\Gamma}^+_\uparrow + \tilde{\Gamma}^+_\downarrow} + \frac{(\tilde{\Gamma}^+_\uparrow \tau_s + 1)(\tilde{\Gamma}^+_\downarrow + \tilde{\Gamma}^-_\downarrow) + (\tilde{\Gamma}^+_\uparrow + \tilde{\Gamma}^-_\uparrow)}{(\tilde{\Gamma}^+_\uparrow \tau_s + 1)\tilde{\Gamma}^+_\downarrow + \tilde{\Gamma}^+_\uparrow} - 1 \right\}^{-1}. \tag{25}$$

The current is then given by the formula

$$I = e \sum_\sigma \tilde{\gamma}_{r\sigma} (n_{\uparrow\downarrow} - \tilde{f}^+_r n_{-\sigma}). \tag{26}$$

The mechanism leading to the suppression of electric current and diodelike behavior, described in Sec. IV, does not apply to the present situation. However, it is still possible to have a diodelike behavior. Consider the same asymmetry of the junction as in Fig. 8. The only difference is that now the discrete level ϵ_d is far below the Fermi level, while $\epsilon_d + U$ is slightly above it in equilibrium. Figures 9(a) and 9(b) show electric current flowing in both magnetic configurations. Consider the case $\Omega = 0$ (no spin-flip processes on the dot). For positive bias, the current begins to flow when $\epsilon_d + U$ crosses the Fermi level of the source electrode. At higher voltages the current is constant, and independent of the bias. The situation is significantly different for negative bias. Now the current vanishes for arbitrary voltage. Thus the diodelike behavior is even much more pronounced than that shown in Fig. 8 and discussed in Ref. 16. The reason for such behavior is as follows. For negative bias, the source electrode is the half-metallic one (for the parameters assumed in Fig. 9), so

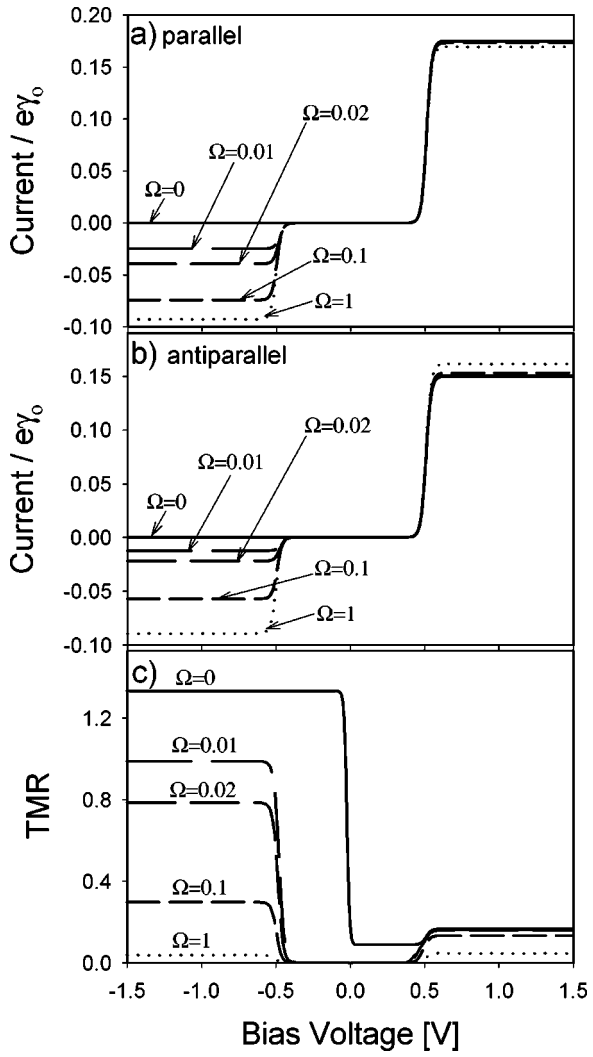

FIG. 9. Electric current in the parallel (a) and antiparallel (b) configurations, and TMR (c) as a function of the bias voltage, calculated for large-U limit with discrete level occupied by a single electron in equilibrium. Different curves correspond to different spin-flip rates, described by the indicated values of the parameter Ω. The other parameters are $\epsilon_d^0 + U = 0.25$ eV, $p_l = 0.4$, $p_r = \epsilon_d^0$, $\alpha = 0.1$, $T = 100$ K, and $x = 0.5$.

only electrons of a particular spin orientation can be injected into the dot—provided that the electron residing at the dot has the opposite spin orientation. If the electron on the dot has the same spin orientation as the electrons in the source electrode, then no tunneling processes can occur. Suppose that, after switching the bias voltage, the electron at the dot has the opposite spin to that of electrons in the half-metallic source electrode. Thus one electron from the source electrode can tunnel to the dot, and then one of the two electrons on the dot (of arbitrary spin orientation) can tunnel further into the drain electrode. When the electron that remains on the dot has the same spin orientation as the electrons in the source electrode, no more tunneling processes can occur, and the current is blocked. Thus, in a stationary state, no current flows for negative bias. As before, spin-flip processes suppress the diodelike behavior, as is also clearly evident from Figs. 9(a) and 9(b).

Differences in the current flowing in both magnetic configuration gives rise to the TMR shown in Fig. 9(c). It is interesting to note that now the enhancement of the TMR due to electron correlations on the dot is for negative bias.

VI. SUMMARY AND CONCLUSIONS

We have considered tunneling through an impurity or a quantum dot with a single discrete level in the presence of Coulomb interaction. Both external electrodes were assumed to be ferromagnetic, and two magnetic configurations were discussed—the parallel and antiparallel configurations. Considerations were limited to the sequential tunneling regime, so quantum interference effects in tunneling,[19,20] such as, e.g., Kondo resonances, were neglected. It was shown that tunneling magnetoresistance, due to rotation of the magnetic moments from antiparallel to parallel alignment, is enhanced by the Coulomb correlations on the dot. The enhancement takes place when the bias is within the range limited by the voltages corresponding to the situations where either the discrete level ϵ_d or $\epsilon_d + U$ crosses the Fermi level of the source electrode.

In asymmetrical junctions the Coulomb correlations on the dot may lead to a suppression of electric current for a particular sign of the bias. The resulting asymmetry in current-voltage characteristics gives rise to a diodelike behavior. This behavior, however, occurs only in the case when spin-flip processes on the dot are sufficiently slow, i.e., when the spin-relaxation time is much longer than the injection time. For faster spin relaxation, diodelike bahavior is generally suppressed by the spin-flip transitions.

The work was supported by The Polish State Committee for Scientific Research through the Research Project No. 5 P03B 091 20.

Note added in proof. Diodelike behavior was recently found also in asymmetric planar junctions [Chshiev *et al.*, cond-mat/0105264].

[1] M. Julliere, Phys. Lett. A **54**, 225 (1975); J. S. Moodera, L. R. Kinder, T. M. Wong, and R. Meservey, Phys. Rev. Lett. **74**, 3273 (1995).

[2] For a review, see S. S. P. Parkin, in *Ultrathin Magnetic Structures*, edited by B. Heinrich and J. A. C. Bland (Springer-Verlag, Berlin, 1994), pp. 148–194.

[3] X. Zhang, B. Z. Li, G. Sun, and F. C. Pu, Phys. Rev. B **56**, 5484 (1997); M. Wilczyński and J. Barnaś, J. Magn. Magn. Mater. **221**, 373 (2000).

[4] J. Barnaś and A. Fert, Phys. Rev. Lett. **80**, 1058 (1998).

[5] J. Barnaś and A. Fert, Europhys. Lett. **44**, 85 (1998); J. Magn. Magn. Mater. **192**, L391 (1999).

[6] S. Takahashi and S. Maekawa, Phys. Rev. Lett. **80**, 1758 (1998); A. Brataas, Yu. V. Nazarov, J. Inoue, and G. E. W. Bauer, Eur. Phys. J. B **9**, 421 (1999); X. H. Wang and A. Brataas, Phys. Rev. Lett. **83**, 5138 (1999).

[7] L. F. Schelp, A. Fert, F. Fettar, P. Holody, S. F. Lee, J. L. Maurice, F. Petroff, and A. Vaures, Phys. Rev. B **56**, R5747 (1997); S. Mitani, H. Fujimori, K. Takanashi, K. Yakushiji, J. G. Ha, S. Takahashi, S. Maekawa, S. Ohnuma, N. Kobayashi, T. Matsumoto, M. Ohnuma, and K. Hono, J. Magn. Magn. Mater. **198-199**, 179 (1999).

[8] For a review, see *Single Charge Tunneling*, Vol. 294 of *NATO Advanced Study Institute, Series B*, Vol. 294 edited by H. Grabert and M. H. Devoret (Plenum Press, New York, 1992).

[9] D. V. Averin and K. K. Likharev, J. Low Temp. Phys. **62**, 345 (1986).

[10] C. W. J. Beenakker, Phys. Rev. B **44**, 1646 (1991); M. Amman, R. Wilkins, E. Ben-Jacob, P. D. Maker, and R. C. Jaklewic, Phys. Rev. B **43**, 1146 (1991).

[11] D. V. Averin, A. N. Korotkov, and K. K. Likhariev, Phys. Rev. B **44**, 6199 (1991).

[12] D. C. Ralph, S. Gueron, C. T. Black, and M. Tinkham, Physica B **280**, 420 (2000).

[13] J. Martinek, J. Barnas, G. Michalek, B. R. Bulka, and A. Fert, J. Magn. Magn. Mater. **207**, L1 (1999).

[14] B. R. Bulka, J. Martinek, G. Michalek, and J. Barnaś, Phys. Rev. B **60**, 12 246 (1999).

[15] J. Barnaś, J. Martinek, G. Michałek, B. Bułka, and A. Fert, Phys. Rev. B **62**, 12 363 (2000).

[16] B. R. Bułka, Phys. Rev. B **62**, 1186 (2000).

[17] L. I. Glazman and K. A. Matveev, Pis'ma Zh. Éksp. Teor. Fiz. 48, 403 (1988) [JETP Lett. **48**, 445 (1988)].

[18] B. Wang, J. Wang, and H. Guo, J. Appl. Phys. **86**, 5094 (1999).

[19] A. Schiller and S. Hershfield, Phys. Rev. B **58**, 14 978 (1998).

[20] A. P. Jauho, N. S. Wingreen, and Y. Meir, Phys. Rev. B **50**, 5528 (1994).